Stationary analysis of a constrained Markov fluid model with two buffers*

Peter Buchholz[1], András Mészáros[2,3], Miklós Telek[2,3]

[1] Technische Universität Dortmund, Dortmund, Germany,

peter.buchholz@cs.tu-dortmund.de

[2] Department of Networked Systems and Services,

Budapest University of Technology and Economics, Hungary

[3] ELKH-BME Information Systems Research Group, Hungary

{meszarosa,telek}@hit.bme.hu

Abstract

We consider Markov fluid models with two infinite buffers, whose fluid rates ensure that the fluid level of buffer 1 is never larger than the one of buffer 2. For the model we derive the system of PDEs describing the transient behavior and expressions for the stationary analysis in the Laplace domain. Examples for the application of the model in the context of network access control are presented. Numerically computed results are compared with detailed simulation results to show that the numerical approach computes the required measures with sufficient accuracy.

Keywords: Markov fluid model, Two infinite fluid buffers, Stationary analysis, Partial differential equations, Laplace transform.

1 Introduction

The analysis of fluid queues has a long tradition in stochastic modeling [6, 7]. Corresponding models are often denoted as Markov modulated fluid models. Originally, single queues or buffers with Markovian arrival processes have been extensively used to model packet switched networks with a large number of sources

*This work is partially supported by the OTKA K-138208 project and the Artificial Intelligence National Laboratory Programme.

[18, 23] or ruin probabilities in financial mathematics [8, 9] among other applications. Analysis of single buffer fluid queues with finite or infinite buffers is well understood. Stationary measures are derived from corresponding results for quasi birth death processes [27, 3, 17, 11], transient results are usually computed in the Laplace domain [4, 12, 5]. Using advanced methods for the numerical inversion of the Laplace transforms [2, 21], the resulting methods for transient analysis are highly accurate and efficient.

Analysis of fluid models with more than one buffer becomes, unfortunately, much more complicated. Different versions of fluid models with two buffers have been introduced in the literature [13, 14, 15]. The classical model considers two fluid buffers $X_1(t)$, $X_2(t)$, where $X_i(t)$ is the level of buffer i at time t, and a finite Markov chain which determines the flow into or out off the buffers. Often it is assumed that flow rates for the first buffer depend on the state of the background Markov chain but not on the filling of the second buffer but rates for the second buffer may depend on both, the state of the background Markov chain and the filling of the first buffer. These models are often denoted as stochastic fluid-fluid models (SFFMs). A specific version of this model describes a tandem of two fluid queues [26, 22]. Fluid models with more than one buffer may be used to model mobile ad hoc networks, maintenance problems, risk processes or environmental systems like coral reefs [8, 14, 24]. Although SFFMs are known for some time, the available operator analytical expression for the stationary distribution of SFFMs [14, 26] usually do not result in numerical algorithms, therefore numerical approximations are applied [10] or only specific sub-classes of the general model are handled [15].

In this paper, we also consider a specific case of a two-dimensional fluid model which is more general than the subclass considered in [15], where fluid rates of both buffers have to be proportional and the background Markov process has a specific structure. In the model analyzed here, two infinite buffers are driven by an arbitrary finite state Markov chain. We assume that in state i of the Markov chain, the level of buffer 1 changes with rate r_i and the level of buffer 2 with rate s_i. Both buffers have an infinite capacity and a lower bound of 0. We assume that the state space of the finite background Markov chain can be decomposed in into two subsets: In state i of the first subset, the level of both buffers increases with an identical rate $r_i = s_i$. In the states of the second subset, the fluid rates are negative, satisfying $r_i \leq s_i$ for all i and, consequently, assuming $X_1(0) = X_2(0) = 0$, we have $X_1(t) \leq X_2(t)$ for $t \geq 0$. The model has applications modeling computer networks and parallel systems. It can, in particular, be used to analyze the behavior of a sequence of leaky buckets with stochastic inputs. However, the current paper focuses mainly on introducing a computational method to analyze the steady state behavior of the model.

A preliminary version of this model, where the background Markov chain has

only two states has been published recently in [16]. The analysis of that model is based on embedded time points, but we could not generalize that analysis approach for more than 2 states. In this paper, we define and analyze the above mentioned model with arbitrary finite background Markov chains based on a fundamentally different analysis approach.

Starting from the partial differential equations describing the transient behaviour of the performance measures of interest, we obtain Laplace transform domain expressions for the stationary measures, which can be conveniently evaluated using numerical inverse Laplace transformation. To validate the results of the numerical algorithm we compare them with simulation results.

The rest of the paper is organized as follows. In the next section we formalize the problem, introduce the necessary notation and describe a typical application. Afterwards the PDEs for the transient behavior are derived, and based on them, the equations for the stationary behavior in Sections 4 and 5. Section 6 describes the solution of the PDEs in the Laplace domain and Section 7 develops an algorithm to compute the required results. In Section 8, we demonstrate the behaviour of the computational method and present results for an example that are compared with simulation results. The paper ends with the conclusions and an outlook of future extensions of the model.

2 The process

Let $X_1(t)$, $X_2(t)$ and $\phi(t)$ be the fluid level in buffer 1, the fluid level of buffer 2, and the state of the irreducible background Markov chain (BMC). The state space is composed of 2 subsets $\mathcal{S} = \mathcal{S}_+ \cup \mathcal{S}_-$. The fluid accumulation is such that

$$\frac{d}{dt}X_1(t) = r_i = \frac{d}{dt}X_2(t) = s_i > 0 \text{ when } \phi(t) = i \in \mathcal{S}_+$$

$$\frac{d}{dt}X_1(t) = r_i \leq s_i < 0 \text{ when } \phi(t) = i \in \mathcal{S}_- \ \& \ X_1(t) > 0 \quad \text{and}$$
$$\frac{d}{dt}X_1(t) = 0 \text{ when } \phi(t) \in \mathcal{S}_- \ \& \ X_1(t) = 0$$

$$\frac{d}{dt}X_2(t) = s_i < 0 \text{ when } \phi(t) = i \in \mathcal{S}_- \ \& \ X_2(t) > 0 \quad \text{and}$$
$$\frac{d}{dt}X_2(t) = 0 \text{ when } \phi(t) \in \mathcal{S}_- \ \& \ X_2(t) = 0.$$

Consequently, $r_i \leq s_i$ for $\forall i \in \mathcal{S}$ and, starting from empty buffers, $X_1(t) \leq X_2(t)$ for $t \geq 0$.

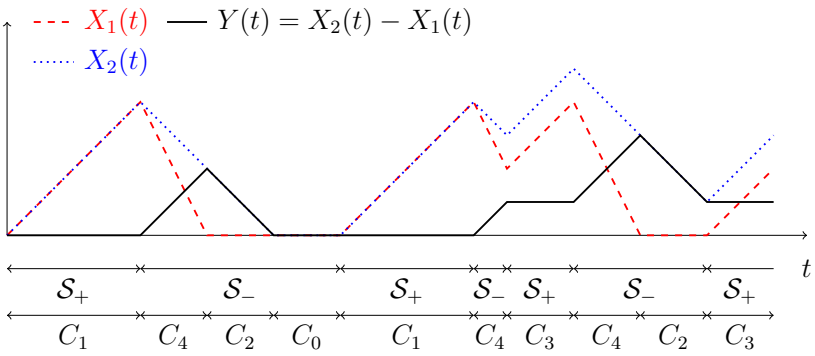

Figure 1: Evolution of the buffer contents

The condition that $s_i < 0$ for $i \in \mathcal{S}_-$, can be relaxed, but we avoid it in this paper in order to maintain a unique $\mathcal{S} = \mathcal{S}_+ \cup \mathcal{S}_-$ decomposition of the state space which applies for both fluid buffers and simplifies the discussion. Additionally, we exclude zero fluid rates for the same reason.

Assuming that the states of the BMC are ordered according to $\mathcal{S}_+$ and $\mathcal{S}_-$, the generator matrix of the modulating BMC can be decomposed as $\mathbf{Q} = \begin{bmatrix} \mathbf{Q}^{++} & \mathbf{Q}^{+-} \\ \mathbf{Q}^{-+} & \mathbf{Q}^{--} \end{bmatrix}$ and the diagonal matrices of the fluid rates associated with buffer 1 and buffer 2 as $\mathbf{R} = \mathrm{diag}(r_1, \ldots, r_{|\mathcal{S}|}) = \begin{bmatrix} \mathbf{R}^+ & \\ & \mathbf{R}^- \end{bmatrix}$ and $\mathbf{S} = \mathrm{diag}(s_1, \ldots, s_{|\mathcal{S}|}) = \begin{bmatrix} \mathbf{S}^+ & \\ & \mathbf{S}^- \end{bmatrix}$, where $\mathbf{R}^+ = \mathbf{S}^+$ have positive diagonal elements and the diagonal elements of $\mathbf{R}^-$ and $\mathbf{S}^-$ are negative. A possible trajectory of the system evolution is depicted in Figure 1.

2.1 Stability condition

The stability of the fluid model is ensured by the stability of buffer 2. Let $\boldsymbol{\pi}$ be the stationary distribution of the irreducible BMC. That is, $\boldsymbol{\pi}\mathbf{Q} = \mathbf{0}$ and $\boldsymbol{\pi}\mathbb{1} = 1$, where $\mathbb{1}$ is the column vector of ones. Buffer 2 is stable when $\boldsymbol{\pi}\mathbf{S}\mathbb{1} < 0$, which we assume to hold in this paper.

3 Motivational example

As a motivating example, in this section we present a tandem queueing system with token bucket servers, which can be mapped to the investigated two buffer fluid model. A token bucket server contains a (packet) buffer, where arriving

packets are waiting for service and a token bucket, which controls the rate of service. The service of packets at the token bucket is assumed to be performed in infinitesimally small parts. The token bucket has a given size b and is filled with tokens with some constant rate ρ. At time t, the next packet in the buffer can be served in zero time if the packet size p is smaller than the $TB(t)$ level of the token bucket at time t, in this case the level of the token bucket is decreased by p. If the size of the next packet to serve is larger than $TB(t)$ then $TB(t)$ bits are served immediately, and the remaining $p - TB(t)$ bits are served at rate ρ. Token buckets are widely used in telecommunication, (e.g., DiffServ [20], the traffic control of Linux kernel [1]) as they provide an efficient way to rate limit communication while decreasing burstiness.

Let us first consider a single token bucket server, where packets arrive to an infinite buffer, whose level at time t is $PB(t)$. As above, let us denote the size of the token bucket by b, the rate of token influx by ρ, and the current level of the bucket by $TB(t)$. Consequently, we have

$$PB(t) \geq 0, \tag{1}$$

$$0 \leq TB(t) \leq b, \tag{2}$$

$$PB(t) = 0 \text{ if } TB(t) > 0, \tag{3}$$

$$TB(t) = 0, \text{ if } PB(t) > 0. \tag{4}$$

From (1) - (4) it follows, that the

$$\bar{X}(t) = PB(t) - TB(t) + b \tag{5}$$

process describes the state of the system completely and that $\bar{X}(t) \geq 0$. $\bar{X}(t)$ is the backlog of the queue shifted by b to ensure non-negativity. When $\bar{X}(t) < b$, then $TB(t) > 0$, thus $PB(t) = 0$. When $\bar{X}(t) = b$, then $PB(t) = TB(t) = 0$, and when $\bar{X}(t) > b$, then $PB(t) > 0$ and $TB(t) = 0$. Let $T_i, \forall i \geq 1$ be the arrival time of the ith packet, S_i the size of the ith packet and $\tau_i = T_i - T_{i-1}, \forall i \geq 1$ their interarrival time with $T_0 = 0$. The evolution of $\bar{X}(t)$ is demonstrated in Figure 2a. To eliminate the jumps from the trajectory, we modify the system behaviour such that the buffer fills with rate 1 instead of instantaneously. Figure 2b demonstrates the evolution of the $X(t)$ process corresponding to this modified system. If S_i and τ_i are Markovian, this modified system can be described by a Markov fluid model whose generator matrix $\mathbf{Q}$ and rate matrix $\mathbf{R}$ have the following structure:

$$\mathbf{Q} = \begin{bmatrix} \mathbf{Q}^{++} & \mathbf{Q}^{+-} \\ \mathbf{Q}^{-+} & \mathbf{Q}^{--} \end{bmatrix}, \quad \mathbf{R} = \begin{bmatrix} \mathbf{I} & \\ & -\rho\mathbf{I} \end{bmatrix}, \tag{6}$$

where $\mathbf{I}$ is the identity matrix whose side is determined by the context, $\mathbf{Q}^{++}$ describes the Markovian transitions while the fluid level increases, $\mathbf{Q}^{+-}$ contains the transitions which concludes the fluid increase period, etc.

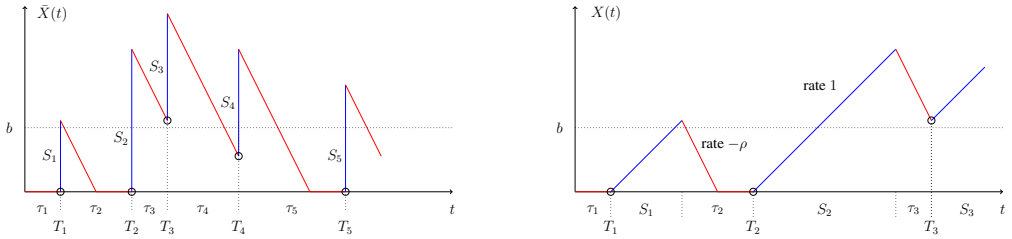

(a) Evolution of $\bar{X}(t)$ (b) Evolution of $X(t)$

Figure 2: Evolution of the single buffer token bucket server

If S_i is independent exponentially distributed with parameter μ, and τ_i is independent exponentially distributed with parameter λ, then

$$\mathbf{Q} = \begin{bmatrix} -\lambda & \lambda \\ \mu & -\mu \end{bmatrix}, \quad \mathbf{R} = \begin{bmatrix} 1 & \\ & -\rho \end{bmatrix}. \tag{7}$$

If S_i is independent phase type distributed with initial vector $\underline{\beta}$ and generator matrix $\mathbf{B}$, and τ_i is independent phase type distributed with initial vector $\underline{\alpha}$ and generator matrix $\mathbf{A}$, then

$$\mathbf{Q} = \begin{bmatrix} \mathbf{A} & \underline{a}\underline{\beta}^T \\ \underline{b}\underline{\alpha}^T & \mathbf{B} \end{bmatrix}, \quad \mathbf{R} = \begin{bmatrix} \mathbf{I} & \\ & -\rho\mathbf{I} \end{bmatrix}, \tag{8}$$

where $\underline{a} = -\mathbf{A}\mathbb{1}$ and $\underline{b} = -\mathbf{B}\mathbb{1}$ and $\mathbb{1}$ is the column vector of ones.

If S_i form a dependent sequence for $i \geq 1$ characterized by a Markov arrival process [25] with matrices $(\mathbf{D_0}, \mathbf{D_1})$ and τ_i form a dependent sequence for $i \geq 1$ characterized by a Markov arrival process with matrices $(\mathbf{G_0}, \mathbf{G_1})$, then

$$\mathbf{Q} = \begin{bmatrix} \mathbf{D_0} \otimes \mathbf{I} & \mathbf{D_1} \otimes \mathbf{I} \\ \mathbf{I} \otimes \mathbf{G_1} & \mathbf{I} \otimes \mathbf{G_0} \end{bmatrix}, \quad \mathbf{R} = \begin{bmatrix} \mathbf{I} & \\ & -\rho\mathbf{I} \end{bmatrix}, \tag{9}$$

where $\otimes$ denotes the Kronecker product of matrices.

If the data served by a first token bucket server is further regulated by a second token bucket server we get the tandem queueing system which is shown in Figure 3a. Server i (for $i \in \{1, 2\}$) has a token bucket with size b_i that fills with rate ρ_i, token level $TB_i(t)$ and packet buffer level $PB_i(t)$ at time t. If $\rho_1 \leq \rho_2$ and $b_1 \leq b_2$, then the presence of server 2 does not change the total delay of the system. In this paper we analyze a fluid model corresponding to the case when $\rho_1 > \rho_2$ and $b_1 \leq b_2$, however, the $\rho_1 \leq \rho_2,\ b_1 > b_2$ case is also tractable with the same methods and corresponds to a fluid model that is identical aside from swapping the indices of the buffers. As for the single buffer case, let us define

$$\bar{X}_1(t) = PB_1(t) - TB_1(t) + b_1,$$
$$\bar{X}_2(t) = PB_2(t) - TB_2(t) + b_2,$$

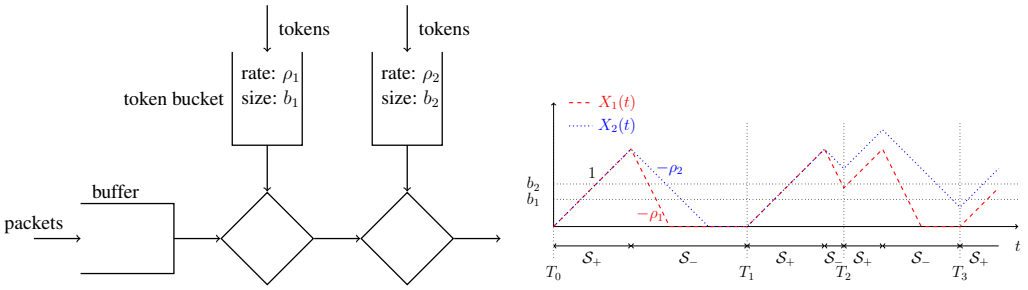

(a) System schema

(b) Evolution of $X_1(t)$ and $X_2(t)$

Figure 3: Tandem queue with two token bucket servers

which are the backlog of server 1 and server 2, shifted by the respective bucket sizes. Similar to before, to eliminate the jumps from the system, we modify its behaviour such that the buffers fills with rate 1 instead of instantaneously and denote the corresponding backlog levels by $X_1(t)$ and $X_2(t)$. The evolution of these processes is demonstrated in Figure 3b.

If S_i and τ_i are Markovian, this modified system can be described by a two buffer Markov fluid model whose generator and rate matrices, $\mathbf{Q}, \mathbf{R}, \mathbf{S}$, have the following structure:

$$\mathbf{Q} = \begin{bmatrix} \mathbf{Q}^{++} & \mathbf{Q}^{+-} \\ \mathbf{Q}^{-+} & \mathbf{Q}^{--} \end{bmatrix}, \quad \mathbf{R} = \begin{bmatrix} \mathbf{I} & \\ & -\rho_1\mathbf{I} \end{bmatrix}, \mathbf{S} = \begin{bmatrix} \mathbf{I} & \\ & -\rho_2\mathbf{I} \end{bmatrix}. \tag{10}$$

This example is a special case of the model introduced in Section 2, where the fluid rates might differ in different positive and negative states.

4 PDE description

In this section we investigate the transient behavior of the system. Let

$$W_i(t,x,y) = \frac{d}{dx}\frac{d}{dy}Pr(\phi(t) = i, X_1(t) < x, X_2(t) < y),$$

$$U_i(t,y) = \frac{d}{dy}Pr(\phi(t) = i, X_1(t) = 0, X_2(t) < y),$$

$$P_i(t) = Pr(\phi(t) = i, X_1(t) = X_2(t) = 0),$$

$$V_i(t,x) = \frac{d}{dx}Pr(\phi(t) = i, X_1(t) < x, X_2(t) < x),$$

where the first 3 measures describe the cases with 0, 1, 2 idle buffers and the last measure describes the fluid accumulation right after both buffers were idle.

By definition, for $i \in \mathcal{S}_+$, $P_i(t) = U_i(t, y) = 0$ and for $i \in \mathcal{S}_-$, $V_i(t, x) = 0$. In Figure 1, C_0 denotes the periods when $X_1(t) = X_2(t) = 0$ (consequently $P_i(t)$ can be positive for $i \in \mathcal{S}_-$), C_1 the ones when $X_1(t) = X_2(t) > 0$ ($V_i(t, x)$ can be positive for $i \in \mathcal{S}_+$), C_2 the ones when $X_1(t) > 0, X_2(t) = 0$ ($U_i(t, y)$ can be positive for $i \in \mathcal{S}_-$), C_3 the ones when $X_2(t) > X_1(t) > 0$ and $\phi(t) \in \mathcal{S}_+$ ($W_i(t, x, y)$ can be positive for $i \in \mathcal{S}_+$), and C_4 the ones when $X_2(t) > X_1(t) > 0$ and $\phi(t) \in \mathcal{S}_-$ ($W_i(t, x, y)$ can be positive for $i \in \mathcal{S}_-$).

To simplify the PDE based analysis, we introduce $Y(t) = X_2(t) - X_1(t)$. $Y(t)$ is such that

$$\begin{aligned}
&\frac{d}{dt}Y(t) = 0 \text{ when } \phi(t) \in \mathcal{S}_+,\\
&\frac{d}{dt}Y(t) = s_i - r_i > 0 \text{ when } \phi(t) = i \in \mathcal{S}_- \ \&\ X_1(t) > 0,\\
&\frac{d}{dt}Y(t) = s_i \text{ when } \phi(t) = i \in \mathcal{S}_- \ \&\ X_1(t) = 0 \ \&\ X_2(t) > 0\\
&\frac{d}{dt}Y(t) = 0 \text{ when } \phi(t) = i \in \mathcal{S}_- \ \&\ X_1(t) = 0 \ \&\ X_2(t) = 0.
\end{aligned}$$

Similar to $\{\phi(t), X_1(t), X_2(t)\}$, $\{\phi(t), X_1(t), Y(t)\}$ is also a Markov fluid model with 2 infinite buffers.

To analyze the $\{\phi(t), X_1(t), Y(t)\}$ system we introduce

$$\tilde{W}_i(t, x, y) = \frac{d}{dx}\frac{d}{dy}Pr(\phi(t) = i, X_1(t) < x, Y(t) < y), \tag{11}$$

$$\tilde{V}_i(t, x) = \frac{d}{dx}Pr(\phi(t) = i, X_1(t) < x, Y(t) = 0), \tag{12}$$

and note that

$$\frac{d}{dy}Pr(\phi(t) = i, X_1(t) = 0, Y(t) < y) = U_i(t, y),$$

$$Pr(\phi(t) = i, X_1(t) = Y(t) = 0) = P_i(t),$$

and $\tilde{V}_i(t, x) = 0$ for $i \in \mathcal{S}_-$.

Below, we present the differential equations governing the $\{\phi(t), X_1(t), Y(t)\}$ system mostly without proofs. These equations can be obtained, e.g., based on [23, 19]. We prove only two of them which are specific to our model.
Let us denote the (i, j) element of $\mathbf{Q}$ as $q_{i,j}$. Then, for $i \in \mathcal{S}_+$, $P_i(t) = 0$ and for $i \in \mathcal{S}_-$

$$\frac{\partial}{\partial t}P_i(t) = \sum_{k \in \mathcal{S}_-} P_k(t)q_{k,i} - s_i U_i(t, 0). \tag{13}$$

For $i \in \mathcal{S}_-$ and $x > 0$, $\tilde{V}_i(t,x) = 0$ and for $i \in \mathcal{S}_+$

$$\frac{\partial}{\partial t}\tilde{V}_i(t,x) + r_i\frac{\partial}{\partial x}\tilde{V}_i(t,x) = \sum_{k\in\mathcal{S}_+}\tilde{V}_k(t,x)q_{k,i} \tag{14}$$

with initial condition

$$r_i\tilde{V}_i(t,0) = \sum_{k\in\mathcal{S}_-}P_k(t)q_{k,i}. \tag{15}$$

For $i \in \mathcal{S}_+$ and $y > 0$, $U_i(t,y) = 0$ and for $i \in \mathcal{S}_-$

$$\frac{\partial}{\partial t}U_i(t,y) + s_i\frac{\partial}{\partial y}U_i(t,y) = \sum_{k\in\mathcal{S}_-}U_k(t,y)q_{k,i} - r_i\tilde{W}_i(t,0,y) \tag{16}$$

For $i \in \mathcal{S}_+$ and $x, y > 0$, $X_1(t)$ increases with rate $r_i > 0$ and $Y(t)$ remains unchanged, that is,

$$\frac{\partial}{\partial t}\tilde{W}_i(t,x,y) + r_i\frac{\partial}{\partial x}\tilde{W}_i(t,x,y) = \sum_{k\in\mathcal{S}}\tilde{W}_k(t,x,y)q_{k,i}, \tag{17}$$

with boundary $\tilde{W}_i(t,x,0) = 0$.

For $i \in \mathcal{S}_-$ and $x, y > 0$, $X_1(t)$ decreases with rate $r_i < 0$ and $Y(t)$ increases with rate $s_i - r_i > 0$, that is,

$$\frac{\partial}{\partial t}\tilde{W}_i(t,x,y) + r_i\frac{\partial}{\partial x}\tilde{W}_i(t,x,y) + (s_i - r_i)\frac{\partial}{\partial y}\tilde{W}_i(t,x,y) = \sum_{k\in\mathcal{S}}\tilde{W}_k(t,x,y)q_{k,i}, \tag{18}$$

and we still need the initial conditions for $\tilde{W}_i(t,x,0)$ when $i \in \mathcal{S}_-$ and $\tilde{W}_i(t,0,y)$ when $i \in \mathcal{S}_+$.

Theorem 1. *For $i \in \mathcal{S}_+$ and $y > 0$*

$$r_i\tilde{W}_i(t,0,y) = \sum_{k\in\mathcal{S}_-}U_k(t,y)q_{k,i} \tag{19}$$

and for $i \in \mathcal{S}_-$ and $x > 0$

$$(s_i - r_i)\tilde{W}_i(t,x,0) = \sum_{k\in\mathcal{S}_+}\tilde{V}_k(t,x)q_{k,i}. \tag{20}$$

Proof. By the definition of $\tilde{W}_i(t,x,y)$ in (11), for $i \in \mathcal{S}_+$ and $y > 0$

$$r_i \tilde{W}_i(t,0,y) = \lim_{\Delta \to 0} \frac{1}{\Delta^2} Pr(\phi(t+\Delta) = i, 0 < X_1(t+\Delta) < r_i\Delta, y < Y(t+\Delta) < y + \Delta). \tag{21}$$

$\phi(t+\Delta) = i, 0 < X_1(t+\Delta) < r_i\Delta, y < Y(t+\Delta) < y+\Delta$ can hold only if there was at least one state transition of the background Markov chain in $(t, t+\Delta)$. Otherwise $X_1(t+\Delta)$ would be larger than $r_i\Delta$.

The probability of more than one state transitions in $(t, t+\Delta)$ vanishes from the differential analysis so we focus on the case when exactly one state transition happen in $(t, t+\Delta)$ and indicate the vanishing term by $\varepsilon(\Delta)$, where $\lim_{\Delta\to 0} \varepsilon(\Delta)/\Delta^2 = 0$.

Starting from $\phi(t) = k \in \mathcal{S}_-, X_1(t) = 0, Y(t) = \gamma$ and having a single state transition from k to i at $t+\tau$ (where $0 < \tau < \Delta$) results in $\phi(t+\Delta) = i, X_1(t+\Delta) = r_i(\Delta - \tau), Y(t+\Delta) = \gamma + s_k\tau$, and the probability density of this state transition is $e^{-q_k\tau} q_{k,i} e^{-q_i(\Delta-\tau)}$, where $q_k = -q_{k,k}$.

That is,

$$\begin{aligned}
&Pr(\phi(t+\Delta) = i, 0 < X_1(t+\Delta) < r_i\Delta, y < Y(t+\Delta) < y+\Delta) \\
&= \sum_{k\in\mathcal{S}_-} \int_{\tau=0}^{\Delta} \int_{\gamma=y-s_k\tau}^{y-s_k\tau+\Delta} U_k(t,\gamma) e^{-q_k\tau} q_{k,i} e^{-q_i(\Delta-\tau)} d\gamma d\tau + \varepsilon(\Delta) \\
&= \sum_{k\in\mathcal{S}_-} q_{k,i} \underbrace{e^{-q_i\Delta}}_{\sim 1} \int_{\tau=0}^{\Delta} \underbrace{\int_{\gamma=y-s_k\tau}^{y-s_k\tau+\Delta} U_k(t,\gamma) d\gamma}_{\sim U_k(t,y)\Delta} \underbrace{e^{(q_i-q_k)\tau}}_{\sim 1} d\tau + \varepsilon(\Delta) \\
&= \sum_{k\in\mathcal{S}_-} q_{k,i} \Delta^2 U_k(t,y) + \varepsilon(\Delta).
\end{aligned}$$

Dividing the expression by Δ^2 and letting $\Delta \to 0$ gives (19).

Similarly, for $i \in \mathcal{S}_-$ and $x > 0$,

$$(s_i - r_i)\tilde{W}_i(t,x,0) = \lim_{\Delta\to 0} \frac{1}{\Delta^2} Pr\Big(\phi(t+\Delta) = i, x < X_1(t+\Delta) < x+\Delta, \\ 0 < Y(t+\Delta) < (s_i - r_i)\Delta\Big) \tag{22}$$

by definition and $\phi(t+\Delta) = i, x < X_1(t+\Delta) < x+\Delta, 0 < Y(t+\Delta) < (s_i - r_i)\Delta$ implies at least one state transition in $(t, t+\Delta)$.

Starting from $\phi(t) = k \in \mathcal{S}_+, X_1(t) = \gamma, Y(t) = 0$ and having a single state transition from k to i at $t + \tau$ (where $0 < \tau < \Delta$) results in $\phi(t + \Delta) = i, X_1(t+\Delta) = \gamma + r_k\tau + r_i(\Delta-\tau), Y(t+\Delta) = (s_i - r_i)(\Delta-\tau)$, and the probability density of this state transition is $e^{-q_k\tau} q_{k,i} e^{-q_i(\Delta-\tau)}$. Following the same steps as before

$$
\begin{aligned}
&Pr(\phi(t+\Delta) = i, x < X_1(t+\Delta) < x + \Delta, 0 < Y(t+\Delta) < (s_i - r_i)\Delta) \\
&= \sum_{k \in \mathcal{S}_+} \int_{\tau=0}^{\Delta} \int_{\gamma=x-r_i\Delta-(r_k-r_i)\tau}^{x-r_i\Delta-(r_k-r_i)\tau+\Delta} \tilde{V}_k(t,\gamma) e^{-q_k\tau} q_{k,i} e^{-q_i(\Delta-\tau)} d\gamma d\tau + \varepsilon(\Delta) \\
&= \sum_{k \in \mathcal{S}_+} q_{k,i} \Delta^2 \tilde{V}_k(t,x) + \varepsilon(\Delta),
\end{aligned}
$$

which gives (20). □

The PDEs can be solved numerical for a transient analysis of the model. For the rest of the paper we derive explicit equations for stationary measures in the Laplace domain, which result in a numerical algorithm for stationary analysis.

5 Stationary behaviour

We introduce the $\mathcal{S}_+$ and $\mathcal{S}_-$ related vectors of the transient measures (e.g., $\mathbf{U}^-(t,y) = \{U_i(t,y)\}$ with $i \in \mathcal{S}_-$)). Using that

$$
\lim_{t\to\infty} \frac{\partial}{\partial t} P_i(t) = \lim_{t\to\infty} \frac{\partial}{\partial t} \tilde{V}_i(t,x) = \lim_{t\to\infty} \frac{\partial}{\partial t} U_i(t,x) = \lim_{t\to\infty} \frac{\partial}{\partial t} W_i(t,x,y) = 0
$$

for all $i \in \mathcal{S}$, we can also introduce the corresponding stationary measures, e.g., $\mathbf{U}^-(y) = \lim_{t\to\infty} \mathbf{U}^-(t,y)$ and obtain the following stationary equations.
From (13), we have

$$
\mathbf{P}^+ = \mathbf{0}\,, \qquad \mathbf{0} = \mathbf{P}^-\mathbf{Q}^{--} - \mathbf{U}^-(0)\mathbf{S}^-. \tag{23}
$$

From (14) and (15), we have

$$
\tilde{\mathbf{V}}^-(x) = \mathbf{0}\,, \qquad \frac{\partial}{\partial x}\tilde{\mathbf{V}}^+(x)\mathbf{R}^+ = \tilde{\mathbf{V}}^+(x)\mathbf{Q}^{++} \tag{24}
$$

with initial condition

$$
\tilde{\mathbf{V}}^+(0)\mathbf{R}^+ = \mathbf{P}^-\mathbf{Q}^{-+}. \tag{25}
$$

From (16), we obtain

$$\mathbf{U}^+(y) = \mathbf{0}\,, \qquad \frac{\partial}{\partial y}\mathbf{U}^-(y)\mathbf{S}^- = \mathbf{U}^-(y)\mathbf{Q}^{--} - \tilde{\mathbf{W}}^-(0,y)\mathbf{R}^-, \tag{26}$$

and from (17) and (19)

$$\frac{\partial}{\partial x}\tilde{\mathbf{W}}^+(x,y)\mathbf{R}^+ = \tilde{\mathbf{W}}^+(x,y)\mathbf{Q}^{++} + \tilde{\mathbf{W}}^-(x,y)\mathbf{Q}^{-+} \tag{27}$$

with initial conditions

$$\tilde{\mathbf{W}}^+(x,0) = \mathbf{0} \quad \text{and} \quad \tilde{\mathbf{W}}^+(0,y)\mathbf{R}^+ = \mathbf{U}^-(y)\mathbf{Q}^{-+}. \tag{28}$$

From (18), we obtain

$$\frac{\partial}{\partial x}\tilde{\mathbf{W}}^-(x,y)\mathbf{R}^- + \frac{\partial}{\partial y}\tilde{\mathbf{W}}^-(x,y)(\mathbf{S}^- - \mathbf{R}^-) = \tilde{\mathbf{W}}^+(x,y)\mathbf{Q}^{+-} + \tilde{\mathbf{W}}^-(x,y)\mathbf{Q}^{--} \tag{29}$$

with initial condition

$$\tilde{\mathbf{W}}^-(x,0)(\mathbf{S}^- - \mathbf{R}^-) = \tilde{\mathbf{V}}^+(x)\mathbf{Q}^{+-}. \tag{30}$$

The stationary behavior of the system satisfies this set of equations, which we simplify as follows. Using (25), the solution of (24) can be written as

$$\tilde{\mathbf{V}}^+(x) = \tilde{\mathbf{V}}^+(0)e^{\mathbf{Q}^{++}(\mathbf{R}^+)^{-1}x} = \mathbf{P}^-\mathbf{Q}^{-+}(\mathbf{R}^+)^{-1}e^{\mathbf{Q}^{++}(\mathbf{R}^+)^{-1}x}. \tag{31}$$

Substituting it into (30), gives

$$\tilde{\mathbf{W}}^-(x,0)(\mathbf{S}^- - \mathbf{R}^-) = \mathbf{P}^-\mathbf{Q}^{-+}(\mathbf{R}^+)^{-1}e^{\mathbf{Q}^{++}(\mathbf{R}^+)^{-1}x}\mathbf{Q}^{+-}. \tag{32}$$

5.1 Directly computable stationary measures

The system definition ensures $X_1(t) \leq X_2(t)$, from which

$$P_i = \lim_{t\to\infty} Pr(\phi(t) = i, X_1(t) = X_2(t) = 0) = \lim_{t\to\infty} Pr(\phi(t) = i, X_2(t) = 0)$$

can be computed from the stationary analysis of buffer 2 in isolation, which is known (e.g. from [27]) and we summarize here for completeness.

Let the $\mathbf{\Psi}_2$ matrix of size $|\mathcal{S}_+| \times |\mathcal{S}_-|$ be the solution of

$$\mathbf{0} = \mathbf{S}^{+-1}\mathbf{Q}^{++}\mathbf{\Psi}_2 + \mathbf{\Psi}_2|\mathbf{S}^-|^{-1}\mathbf{Q}^{--} + \mathbf{\Psi}_2|\mathbf{S}^-|^{-1}\mathbf{Q}^{-+}\mathbf{\Psi}_2 + \mathbf{S}^{+-1}\mathbf{Q}^{+-} \tag{33}$$

and $\mathbf{K}_2 = \mathbf{S}^{+-1}\mathbf{Q}^{++} + \mathbf{\Psi}_2|\mathbf{S}^-|^{-1}\mathbf{Q}^{-+}$. Then vector $\mathbf{P}^-$ is the solution of

$$\mathbf{P}^-(\mathbf{Q}^{--} + \mathbf{Q}^{-+}\mathbf{\Psi}_2) = \mathbf{0} \tag{34}$$

with normalizing condition

$$\mathbf{P}^-\mathbb{1} + \mathbf{P}^-\mathbf{Q}^{-+}(-\mathbf{K}_2)^{-1}(\mathbf{S}^{+-1}\mathbb{1} + \mathbf{\Psi}_2|\mathbf{S}^-|^{-1}\mathbb{1}) = 1. \tag{35}$$

For $i \in \mathcal{S}_-$, let $L_i = \lim_{t\to\infty} Pr(\phi(t) = i, X_1(t) = 0)$ be the stationary probability that buffer 1 is empty, and let $\mathbf{L}^- = \{L_i\}$ (for $i \in \mathcal{S}_-$). $\mathbf{L}^-$ can be computed from $\mathbf{Q}$ and $\mathbf{R}$ in a similar way as $\mathbf{P}^-$ is computed from $\mathbf{Q}$ and $\mathbf{S}$.

The results of the independent analysis of buffer 1 and 2 are related by

$$\begin{aligned} L_i &= \lim_{t\to\infty} Pr(\phi(t) = i, X_1(t) = 0) \\ &= \lim_{t\to\infty} Pr(\phi(t) = i, X_1(t) = X_2(t) = 0) + Pr(\phi(t) = i, X_1(t) = 0, X_2(t) > 0) \\ &= P_i + \int_0^\infty U_i(y)dy. \end{aligned}$$

That is

$$\mathbf{L}^- = \mathbf{P}^- + \int_0^\infty \mathbf{U}^-(y)dy, \tag{36}$$

where $\mathbf{P}^-$ and $\mathbf{L}^-$ are computed as described above.

6 LT domain

We look for the solution of the PDEs in Laplace transform domain. Due to $\mathbf{P}^+ = \mathbf{0}$, $\mathbf{U}^+(y) = \mathbf{0}$ and $\tilde{\mathbf{V}}^-(x) = \mathbf{0}$ we omit the superscript of $\mathbf{P}^-$, $\mathbf{U}^-(y)$ and $\tilde{\mathbf{V}}^+(x)$.

Applying x to s and y to z Laplace transforms for $\mathbf{U}^*(z) = \int_0^\infty e^{-yz}\mathbf{U}(y)dy$, $\mathbf{V}^*(s) = \int_0^\infty e^{-xs}\mathbf{V}(x)dx$, $\mathbf{W}^{+,**}(s) = \int_0^\infty\int_0^\infty e^{-yz}e^{-xs}\mathbf{W}^+(x,y)dxdy$ and $\mathbf{W}^{-,**}(s) = \int_0^\infty\int_0^\infty e^{-yz}e^{-xs}\mathbf{W}^-(x,y)dxdy$ give the following expressions.

Theorem 2. *$\tilde{\mathbf{W}}^{-,**}(s,z)$ and $\tilde{\mathbf{W}}^{+,**}(s,z)$ satisfy*

$$\begin{aligned} \tilde{\mathbf{W}}^{-,**}(s,z) = \Big(\mathbf{U}^*(z)\Big(-z\mathbf{S}^- + \mathbf{Q}^-(s)\Big) + \mathbf{P}\mathbf{Q}^-(s)\Big) \\ \Big(s\mathbf{R}^- + z(\mathbf{S}^- - \mathbf{R}^-) - \mathbf{Q}^-(s)\Big)^{-1} \end{aligned} \tag{37}$$

and

$$\tilde{\mathbf{W}}^{+,**}(s,z) = \Big(\tilde{\mathbf{W}}^{-,**}(s,z) + \mathbf{U}^*(z)\Big)\mathbf{Q}^{-+}\Big(s\mathbf{R}^+ - \mathbf{Q}^{++}\Big)^{-1}, \tag{38}$$

where $\mathbf{Q}^-(s) = \mathbf{Q}^{--} + \mathbf{Q}^{-+}\Big(s\mathbf{R}^+ - \mathbf{Q}^{++}\Big)^{-1}\mathbf{Q}^{+-}$.

Proof. Using the notation

$$\tilde{\mathbf{W}}^{-,*\cdot}(s,0) = \int_0^\infty e^{-xs}\mathbf{W}^-(x,0)dx,$$
$$\tilde{\mathbf{W}}^{-,\cdot *}(0,z) = \int_0^\infty e^{-yz}\mathbf{W}^-(0,y)dy,$$

from (26) and (23), we have

$$z\mathbf{U}^*(z)\mathbf{S}^- - \underbrace{\mathbf{U}(0)\mathbf{S}^-}_{\mathbf{PQ}^{--}} = \mathbf{U}^*(z)\mathbf{Q}^{--} - \tilde{\mathbf{W}}^{-,\cdot *}(0,z)\mathbf{R}^-$$

and consequently

$$\tilde{\mathbf{W}}^{-,\cdot *}(0,z)\mathbf{R}^- = -\mathbf{U}^*(z)\Big(z\mathbf{S}^- - \mathbf{Q}^{--}\Big) + \mathbf{PQ}^{--}. \tag{39}$$

From (31)

$$\tilde{\mathbf{V}}^*(s) = \tilde{\mathbf{V}}^+(0)\Big(s\mathbf{I} - \mathbf{Q}^{++}(\mathbf{R}^+)^{-1}\Big)^{-1} = \mathbf{PQ}^{-+}(\mathbf{R}^+)^{-1}\Big(s\mathbf{I} - \mathbf{Q}^{++}(\mathbf{R}^+)^{-1}\Big)^{-1}$$
$$= \mathbf{PQ}^{-+}\Big(s\mathbf{R}^+ - \mathbf{Q}^{++}\Big)^{-1}. \tag{40}$$

From (28), we write

$$\tilde{\mathbf{W}}^{+,\cdot *}(0,z)\mathbf{R}^+ = \mathbf{U}^*(z)\mathbf{Q}^{-+}. \tag{41}$$

Using (41) and (27), we have

$$\begin{aligned} s\tilde{\mathbf{W}}^{+,**}(s,z)\mathbf{R}^+ - \tilde{\mathbf{W}}^{+,\cdot *}(0,z)\mathbf{R}^+ &= \tilde{\mathbf{W}}^{+,**}(s,z)\mathbf{Q}^{++} + \tilde{\mathbf{W}}^{-,**}(s,z)\mathbf{Q}^{-+} \\ s\tilde{\mathbf{W}}^{+,**}(s,z)\mathbf{R}^+ - \mathbf{U}^*(z)\mathbf{Q}^{-+} &= \tilde{\mathbf{W}}^{+,**}(s,z)\mathbf{Q}^{++} + \tilde{\mathbf{W}}^{-,**}(s,z)\mathbf{Q}^{-+} \\ \tilde{\mathbf{W}}^{+,**}(s,z)\Big(s\mathbf{R}^+ - \mathbf{Q}^{++}\Big) &= \tilde{\mathbf{W}}^{-,**}(s,z)\mathbf{Q}^{-+} + \mathbf{U}^*(z)\mathbf{Q}^{-+}. \end{aligned} \tag{42}$$

which results in (38).

From (30) and (40), we obtain

$$\tilde{\mathbf{W}}^{-,*\cdot}(s,0)(\mathbf{S}^- - \mathbf{R}^-) = \tilde{\mathbf{V}}^*(s)\mathbf{Q}^{+-} = \mathbf{PQ}^{-+}\Big(s\mathbf{R}^+ - \mathbf{Q}^{++}\Big)^{-1}\mathbf{Q}^{+-} \tag{43}$$

and from (29)

$$\Big(s\tilde{\mathbf{W}}^{-,**}(s,z) - \tilde{\mathbf{W}}^{-,\cdot *}(0,z)\Big)\mathbf{R}^- + \Big(z\tilde{\mathbf{W}}^{-,**}(s,z) - \tilde{\mathbf{W}}^{-,*\cdot}(s,0)\Big)(\mathbf{S}^- - \mathbf{R}^-)$$
$$= \tilde{\mathbf{W}}^{+,**}(s,z)\mathbf{Q}^{+-} + \tilde{\mathbf{W}}^{-,**}(s,z)\mathbf{Q}^{--}. \tag{44}$$

Substituting (39) and (43) into (44) gives

$$s\tilde{\mathbf{W}}^{-,**}(s,z)\mathbf{R}^- + \mathbf{U}^*(z)\Big(z\mathbf{S}^- - \mathbf{Q}^{--}\Big) - \mathbf{P}\mathbf{Q}^{--} + z\tilde{\mathbf{W}}^{-,**}(s,z)(\mathbf{S}^- - \mathbf{R}^-)$$
$$- \mathbf{P}\mathbf{Q}^{-+}\Big(s\mathbf{R}^+ - \mathbf{Q}^{++}\Big)^{-1}\mathbf{Q}^{+-} = \tilde{\mathbf{W}}^{+,**}(s,z)\mathbf{Q}^{+-} + \tilde{\mathbf{W}}^{-,**}(s,z)\mathbf{Q}^{--} \quad (45)$$

and

$$\tilde{\mathbf{W}}^{-,**}(s,z)\Big(s\mathbf{R}^- + z(\mathbf{S}^- - \mathbf{R}^-) - \mathbf{Q}^{--}\Big) = \tilde{\mathbf{W}}^{+,**}(s,z)\mathbf{Q}^{+-}$$
$$- \mathbf{U}^*(z)\Big(z\mathbf{S}^- - \mathbf{Q}^{--}\Big) + \mathbf{P}\mathbf{Q}^{--} + \mathbf{P}\mathbf{Q}^{-+}\Big(s\mathbf{R}^+ - \mathbf{Q}^{++}\Big)^{-1}\mathbf{Q}^{+-}. \quad (46)$$

Finally, substituting (38) into (46) gives

$$\tilde{\mathbf{W}}^{-,**}(s,z)\Big(s\mathbf{R}^- + z(\mathbf{S}^- - \mathbf{R}^-) - \mathbf{Q}^{--}\Big)$$
$$= \Big(\Big(\tilde{\mathbf{W}}^{-,**}(s,z) + \mathbf{U}^*(z)\Big)\mathbf{Q}^{-+}\Big(s\mathbf{R}^+ - \mathbf{Q}^{++}\Big)^{-1}\Big)\mathbf{Q}^{+-}$$
$$- \mathbf{U}^*(z)\Big(z\mathbf{S}^- - \mathbf{Q}^{--}\Big) + \mathbf{P}\mathbf{Q}^{--} + \mathbf{P}\mathbf{Q}^{-+}\Big(s\mathbf{R}^+ - \mathbf{Q}^{++}\Big)^{-1}\mathbf{Q}^{+-}, \quad (47)$$

$$\tilde{\mathbf{W}}^{-,**}(s,z)\Big(s\mathbf{R}^- + z(\mathbf{S}^- - \mathbf{R}^-) - \mathbf{Q}^{--} - \mathbf{Q}^{-+}\Big(s\mathbf{R}^+ - \mathbf{Q}^{++}\Big)^{-1}\mathbf{Q}^{+-}\Big)$$
$$= \mathbf{U}^*(z)\mathbf{Q}^{-+}\Big(s\mathbf{R}^+ - \mathbf{Q}^{++}\Big)^{-1}\mathbf{Q}^{+-} - \mathbf{U}^*(z)\Big(z\mathbf{S}^- - \mathbf{Q}^{--}\Big)$$
$$+ \mathbf{P}\mathbf{Q}^{--} + \mathbf{P}\mathbf{Q}^{-+}\Big(s\mathbf{R}^+ - \mathbf{Q}^{++}\Big)^{-1}\mathbf{Q}^{+-} \quad (48)$$

and

$$\tilde{\mathbf{W}}^{-,**}(s,z)\Big(s\mathbf{R}^- + z(\mathbf{S}^- - \mathbf{R}^-) - \mathbf{Q}^-(s)\Big)$$
$$= \mathbf{U}^*(z)\Big(-z\mathbf{S}^- + \mathbf{Q}^-(s)\Big) + \mathbf{P}\mathbf{Q}^-(s). \quad (49)$$

Equation (49) results in (37). □

Remark 1. *For $s = 0$, $\mathbf{Q}^-(0) = \mathbf{Q}^{--} + \mathbf{Q}^{-+}\big(-\mathbf{Q}^{++}\big)^{-1}\mathbf{Q}^{+-}$ is the generator of the CTMC which is the BMC restricted to $\mathcal{S}_-$. This way the dominant eigenvalue of $\mathbf{Q}^-(0)$ is 0 and all other eigenvalues have negative real parts. For a real positive s, $\mathbf{Q}^-(s)$ is the generator of a transient CMTC with all eigenvalues having negative real parts and the dominant one is real and unique with its real part. For $Re(s) > 0$, all eigenvalues of $\mathbf{Q}^-(s)$ have negative real part.*

The only unknown which we still need for applying Theorem 2 is $\mathbf{U}^*(z)$.

6.1 Analysis of $\mathbf{U}^*(z)$

We compute $\mathbf{U}^*(z)$ based on the property that (37) is analytic for $Re(s) > 0$. For a fixed z and $i = 1, \ldots, |\mathcal{S}_-|$, let s_i be the ith solutions of

$$\det\left(\mathbf{F}^*(s,z)\right) = 0 \tag{50}$$

with positive real part, where $\mathbf{F}^*(s,z) = s\mathbf{R}^- + z(\mathbf{S}^- - \mathbf{R}^-) - \mathbf{Q}^-(s)$.

Let $\mathbf{u}_i$ be the right eigenvector of $\mathbf{F}^*(s_i,z)$ associated with eigenvalue 0, that is, $\mathbf{u}_i$ satisfying

$$\mathbf{F}^*(s_i,z)\mathbf{u}_i = \mathbf{0}. \tag{51}$$

According to (37), $\tilde{\mathbf{W}}^{-,**}(s,z)$ is analytic at s_i, when the effect of the zero eigenvalue is eliminated by the fact that $\mathbf{u}_i$ is orthogonal to $\Big(\mathbf{U}^*(z)\Big(- z\mathbf{S}^- + \mathbf{Q}^-(s_i)\Big) + \mathbf{P}\mathbf{Q}^-(s_i)\Big)$, that is,

$$\Big(\mathbf{U}^*(z)\Big(- z\mathbf{S}^- + \mathbf{Q}^-(s_i)\Big) + \mathbf{P}\mathbf{Q}^-(s_i)\Big)\mathbf{u}_i = 0 \tag{52}$$

for $\forall i \in \{1, \ldots, |\mathcal{S}_-|\}$, which gives $|\mathcal{S}_-|$ equations for the $|\mathcal{S}_-|$ elements of $\mathbf{U}^*(z)$.

7 The proposed computational method

In the following we present a computational method for the stationary probability measures of the fluid model. From (23), (24), and (26) we have $\mathbf{P}^+ = \mathbf{0}$, $\tilde{\mathbf{V}}^-(x) = \mathbf{0}$, and $\tilde{\mathbf{U}}^+(y) = \mathbf{0}$, respectively. The rest of the corresponding probability measures can be computed as follows.

7.1 Procedure for computing $\mathbf{P}^-$ and $\tilde{\mathbf{V}}^+(x)$

1. Compute $\mathbf{P}^-$ as the solution of the linear system (34) with normalizing condition (35).

2. Compute $\tilde{\mathbf{V}}^+(x)$ based on (31).

$\mathbf{P}^-$ and $\tilde{\mathbf{V}}^+(x)$ are computed directly without applying Laplace transform description.

7.2 Procedure for computing $\mathbf{U}^*(z)$

To compute $\mathbf{U}^*(z)$ for a given z perform the following steps (based on the analysis from Section 6.1).

1. Based on (50), compute the $|\mathcal{S}_-|$ roots of $\det\left(\mathbf{F}^*(s,z)\right) = 0$ with positive real part, denoted as $s_1, \ldots, s_{|\mathcal{S}_-|}$
2. For all $i \in \{1, \ldots, |\mathcal{S}_-|\}$ compute $\mathbf{u}_i$ ($\mathbf{u}_i \neq \mathbf{0}$) based on $\mathbf{F}^*(s_i, z)\mathbf{u}_i = \mathbf{0}$, according to (51).
3. Following (52), compute $\mathbf{U}^*(z)$ from the set of $|\mathcal{S}_-|$ equations: $\Big(\mathbf{U}^*(z)\Big(- z\mathbf{S}^- + \mathbf{Q}^-(s_i)\Big) + \mathbf{P}\mathbf{Q}^-(s_i)\Big)\mathbf{u}_i = 0$ for $i = 1, \ldots, |\mathcal{S}_-|$.

7.3 Procedure for computing $\tilde{\mathbf{W}}^{+,**}(s,z)$ and $\tilde{\mathbf{W}}^{-,**}(s,z)$

To compute $\tilde{\mathbf{W}}^{**}(s,z)$ for a given s and z perform the following steps.

1. Compute $\mathbf{U}^*(z)$ for the given z according to Section 7.2.
2. Based on s, z, and $\mathbf{U}^*(z)$ compute $\tilde{\mathbf{W}}^{-,**}(s,z)$ using (37).
3. Based on s, z, $\mathbf{U}^*(z)$, and $\tilde{\mathbf{W}}^{-,**}(s,z)$ compute $\tilde{\mathbf{W}}^{+,**}(s,z)$ using (38).

7.4 Computation of $\mathbf{U}^-(y)$ and $\tilde{\mathbf{W}}(x,y)$

$\mathbf{U}^-(y)$ is obtained from $\mathbf{U}^*(z)$ using one dimensional numerical inverse Laplace transformation, while $\tilde{\mathbf{W}}(x,y)$ is obtained from $\tilde{\mathbf{W}}^{+,**}(s,z)$ and $\tilde{\mathbf{W}}^{-,**}(s,z)$ using two dimensional numerical inverse Laplace transformation. Efficient numerical inverse Laplace transformation (NILT) procedures of order n require the evaluation of the Laplace transform function in n points with positive real part in one dimension and in n^2 points with positive real part in two dimensions [2, 21]. That is, the computation of $\mathbf{U}^-(y)$ requires the evaluation of $\mathbf{U}^*(z)$ in n points and the computation of $\tilde{\mathbf{W}}(x,y)$ the evaluation of $\tilde{\mathbf{W}}^{+,**}(s,z)$ and $\tilde{\mathbf{W}}^{-,**}(s,z)$ in $n \times n$ points, such that the more expensive computation of $\mathbf{U}^*(z)$ according to Section 7.2, is performed only n times. Consequently, the calculation of $\tilde{\mathbf{W}}(x,y)$ is still the dominant factor in the overall computational cost.

8 Numerical examples

We present two different kinds of examples. First, we describe the detailed analysis of an artificial model where we perform a detailed analysis of the numerical results. Afterwards, we analyze a tandem system of two token buckets.

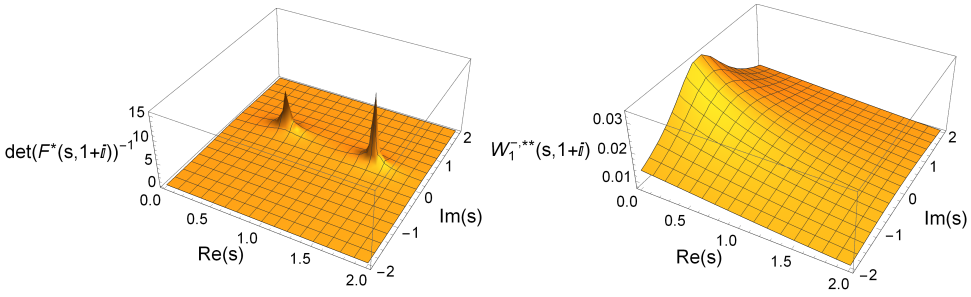

(a) (b)

Figure 4: $|det\left((\mathbf{F}^*(s,z))^{-1}\right)|$ and $|\tilde{\mathbf{W}}^{-,**}(s,z)|$ as a function of s at $z = 1 + \mathrm{i}$

8.1 A detailed numerical demonstration of the method

We first demonstrate the computation of $\mathbf{U}^*(z)$ according to Section 6.1 and verify the LT domain formulas through a comparison with the results of a fluid simulator. We consider the fluid model with

$$\mathbf{Q} = \begin{bmatrix} -4 & 1.7 & 1.1 & 1.2 \\ 3.6 & -5 & 0.5 & 0.9 \\ 0.3 & 1.5 & -2 & 0.2 \\ 1.5 & 0.5 & 1 & -3 \end{bmatrix}, \quad \mathbf{R} = \begin{bmatrix} 1 & 0 & 0 & 0 \\ 0 & 2 & 0 & 0 \\ 0 & 0 & -2 & 0 \\ 0 & 0 & 0 & -3 \end{bmatrix}, \quad \mathbf{S} = \begin{bmatrix} 1 & 0 & 0 & 0 \\ 0 & 2 & 0 & 0 \\ 0 & 0 & -1.5 & 0 \\ 0 & 0 & 0 & -2 \end{bmatrix}.$$

8.1.1 Calculating $\mathbf{U}^*(z)$

The computation of $\mathbf{U}^*(z)$ is based on the fact that $\tilde{\mathbf{W}}^{-,**}(s,z)$ has to be analytic for $Re(s) > 0$. We demonstrate the application of this constraint in the following. Figure 4a depicts the effect of the roots of (50). Figure 4a plots the absolute value of $det\left(\mathbf{F}^*(s,z)^{-1}\right)$ for different s values with fixed $z = 1 + \mathrm{i}$, where i denotes the imaginary unit. The singularities in this figure at $s_1 = 0.54 + 0.41\mathrm{i}$ and $s_2 = 1.51 + 0.29\mathrm{i}$ indicate the points where $\mathbf{F}^*(s,z)^{-1}$ is not analytic.

The fact that $\tilde{\mathbf{W}}^{-,**}(s,z)$ is analytic in these points as well, gives two constraints for $\mathbf{U}^*(z)$ according to (52), from which $\mathbf{U}^*(1+\mathrm{i}) = [0.0180 - 0.00957\mathrm{i}, 0.0118 - 0.0596\mathrm{i}]$. Using this, $\tilde{\mathbf{W}}^{-,**}(s, 1+\mathrm{i})$ can be obtained from (37) and results in the smooth analytic function whose absolute value is depicted in Figure 4b.

8.1.2 Implementation note

The procedure to compute $\mathbf{U}^*(z)$ utilizes that (50) has $|\mathcal{S}_-|$ distinct solutions with positive real part. Theoretically, it might happen that some of those solutions coincide. In the example it occurs at $z = 2.7098 + 7.6646\mathrm{i}$, where $s = 1.68395 +$

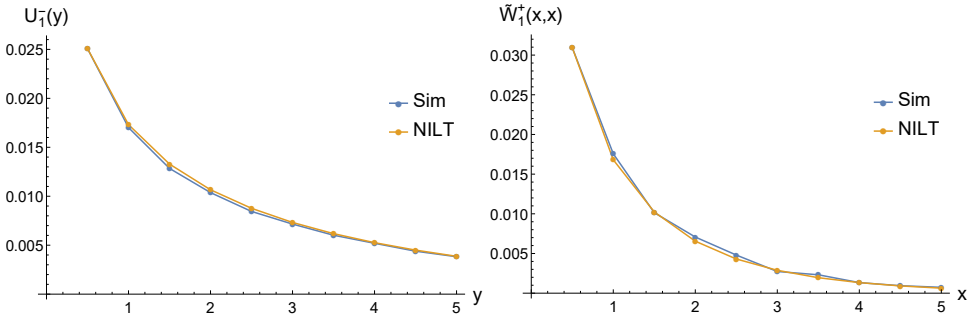

(a) $\mathbf{U}_1^-(y)$ (b) $\tilde{\mathbf{W}}_1^+(x,x)$

Figure 5: The results of simulation and NILT for $\mathbf{U}_1^-(y)$ and $\tilde{\mathbf{W}}_1^+(x,x)$

$2.33178\mathrm{i}$ is the root of (50) with multiplicity 2. In this case, we do not have $|\mathcal{S}_-| = 2$ equations for the $|\mathcal{S}_-| = 2$ elements of $\mathbf{U}^*(z)$, and $\mathbf{U}^*(z)$ cannot be computed.

The existence of rare (zero measure) z values where $\mathbf{U}^*(z)$ is not available does not inhibit the application of the proposed numerical procedure, because the points where $\mathbf{U}^*(z)$ needs to be evaluated depends on the applied NILT method. If the problem of coinciding solutions appears in the computation with order n NILT one can apply order $n+1$ NILT which evaluates $\mathbf{U}^*(z)$ in different points where $\mathbf{U}^*(z)$ is available with high probability.

The problem of coinciding solutions never appeared during our numerical analysis. Indeed, it was challenging find $z = 2.7098 + 7.6646\mathrm{i}$, which exemplifies the existence of this problem.

8.1.3 Comparison with simulation

To verify the procedures in Section 7, we implemented a fluid simulator for the investigated model in Matlab. We used 100,000 runs of 1000 in model seconds (out of which the first 100 seconds are discarded as warm-up phase) and approximated the stationary pdf of the system using a resolution of $\Delta x = \Delta y = 0.1$.

To get comparable results from the analytical formulas, we applied numerical inverse Laplace transformation (NILT) on the Laplace domain expressions for $\mathbf{U}^*(z)$, $\tilde{\mathbf{W}}^{-,**}(s,z)$, and $\tilde{\mathbf{W}}^{+,**}(s,z)$ using the order 30 CME method presented in [21]. As a demonstration, the results for the first element of $\mathbf{U}^-(y)$ and of $\tilde{\mathbf{W}}^+(x,y)$ with $y = x$, denoted as $\mathbf{U}_1^-(y)$ and $\tilde{\mathbf{W}}_1^+(x,x)$, respectively, are shown in Figure 5. The curves obtained from NILT show good correspondence with the simulation results. All other evaluated $\mathbf{U}^-(y)$, $\tilde{\mathbf{W}}^-(x,y)$ and $\tilde{\mathbf{W}}^+(x,y)$ curves indicate similar accuracy.

	$Pr(\tilde{X}_1 > b_1 \vee \tilde{X}_2 > b_2)$	
b_1	simulation	NILT
0.5	0.412	0.413
1.0	0.271	0.273
1.5	0.181	0.183
2.5	0.080	0.082
4.0	0.023	0.024

Table 1: Results for the model with two token buffers and uncorrelated arrivals.

8.2 A Tandem of Leaky Buckets

We consider an example of a tandem of token buckets shown in Fig. 3a and described in Section 3. Two variants of the model are analyzed. In the first variant, we assume that inter-arrival times are hyper-exponentially distributed and the amount of work (i.e., the packet size) is Erlang-2 distributed resulting in generator matrix

$$\mathbf{Q} = \left(\begin{array}{cc|cc} -1 & 0 & 1 & 0 \\ 0 & -3 & 3 & 0 \\ \hline 0 & 0 & -2 & 2 \\ 1 & 1 & 0 & -2 \end{array}\right).$$

We analyze the model with two token buffers with $\rho_1 = 2$, $\rho_2 = 1$, varying b_1 and $b_2 = 2 * b_1$. As a measure we consider $Pr(\tilde{X}_1 > b_1 \vee \tilde{X}_2 > b_2)$, the probability that load has to wait due to an empty bucket. The NILT calculation using our Wolfram Mathematica implementation takes around 1 second per data point for this example. Results for different values of b_1 are shown in Tab. 1.

As a second version of the example, we analyze the model with generator matrix

$$\mathbf{Q} = \left(\begin{array}{cc|cccc} -1 & 0 & 1 & 0 & 0 & 0 \\ 0 & -3 & 0 & 0 & 3 & 0 \\ \hline 0 & 0 & -2 & 2 & 0 & 0 \\ 1.8 & 0.2 & 0 & -2 & 0 & 0 \\ 0 & 0 & 0 & 0 & -2 & 2 \\ 0.2 & 1.8 & 0 & 0 & 0 & -2 \end{array}\right).$$

In this case, the service and inter-arrival times are distributed as in the first example but inter-arrival times are positively correlated. The NILT calculation takes around 5 seconds per data point for this larger example. The corresponding results are presented in Tab. 2. It can be seen that the positive correlation results in

	$Pr(\tilde{X}_1 > b_1 \vee \tilde{X}_2 > b_2)$	
b_1	simulation	NILT
0.5	0.450	0451
1.0	0.340	0.341
1.5	0.260	0.262
2.5	0.153	0.155
4.0	0.068	0.070

Table 2: Results for the model with two token buffers and correlated arrivals.

a much higher probability that the token buffer is empty and load has to wait for access to the system.

Examples like the one we present here can be applied to configure access control by sequences of leaky buckets.

9 Conclusion

The paper presents a numerical analysis method for a special Markov fluid model with two fluid buffers of infinite capacity. The proposed computational procedure provides a Laplace transform domain description of the model behaviour using a numerical inverse transformation method. It is one of the first approaches to compute stationary measures of fluid models with more than one buffer explicitly.

Our longer term research goal is to relax the model restrictions applied in this work and to find an analysis approach for the stationary solution of Markov fluid models with two fluid buffers and general fluid rates. Furthermore, we work on different applications of the model for computer networks and maintenance problems.

References

[1] tc(8) - Linux manual page. `https://man7.org/linux/maxn-pages/man8/tc.8.htmll`. Accessed: 2023-08-09.

[2] J. Abate and W. Whitt. A Unified Framework for Numerically Inverting Laplace Transforms. *INFORMS Journal on Computing*, 18(4):408–421, Fall 2006.

[3] S. Ahn, J. Jeon, and V. Ramaswami. Steady state analysis of finite fluid flow models using finite QBDs. *Queueing Systems*, 49(3):223–259, Apr 2005.

[4] S. Ahn and V. Ramaswami. Efficient algorithms for transient analysis of stochastic fluid flow models. *Journal of Applied Probability*, 42(2):531–549, 2005.

[5] S. A.-D. Almousa, G. Horváth, and M. Telek. Transient analysis of piecewise homogeneous Markov fluid models. *Annals of Operations Research*, 310:333–353, 2022.

[6] D. Anick, D. Mitra, and M. M. Sondhi. Stochastic Theory of a Data-Handling System. *Bell Sys. Thech. J*, 61(8):1871–1894, Oct 1982.

[7] S. Asmussen. Stationary distributions for fluid flow models with or without brownian noise. *Communications in statistics. Stochastic models*, 11(1):21–49, 1995.

[8] A. Badescu, L. Breuer, A. Da Silva Soares, G. Latouche, M.-A. Remiche, and D. Stanford. Risk processes analyzed as fluid queues. *Scandinavian Actuarial Journal*, 2005(2):127–141, 2005.

[9] A. Badescu, S. Drekic, and D. Landriault. On the analysis of a multi-threshold Markovian risk model. *Scandinavian Actuarial Journal*, 2007(4):248–260, 2007.

[10] N. Bean, A. Lewis, G. T. Nguyen, M. M. O'Reilly, and V. Sunkara. A discontinuous galerkin method for approximating the stationary distribution of stochastic fluid-fluid processes. *Methodology and Computing in Applied Probability*, 24(4):2823–2864, 2022.

[11] N. Bean, G. Nguyen, and F. Poloni. Doubling algorithms for stationary distributions of fluid queues: A probabilistic interpretation. *Performance Evaluation*, 125:1–20, 2018.

[12] N. Bean, M. O'Reilly, and P. Taylor. Algorithms for the Laplace-Stieltjes transforms of first return times for stochastic fluid flows. *Methodology and Computing in Applied Probability*, 10:381–408, 09 2008.

[13] N. G. Bean and M. M. O'Reilly. A stochastic two-dimensional fluid model. *Stochastic Models*, 29(1):31–63, 2013.

[14] N. G. Bean and M. M. O'Reilly. The stochastic fluid-fluid model: A stochastic fluid model driven by an uncountable-state process, which is a

stochastic fluid model itself. *Stochastic Processes and their Applications*, 124(5):1741–1772, 2014.

[15] N. G. Bean, M. M. O'Reilly, and Z. Palmowski. Matrix-analytic methods for the analysis of stochastic fluid-fluid models. *Stochastic Models*, 38(3):416–461, 2022.

[16] P. Buchholz, A. Meszaros, and M. Telek. Analysis of a two-state markov fluid model with 2 buffers. In *27th International Conference on Analytical & Stochastic Modelling Techniques & Applications (ASMTA)*, Florence,Italy, 2023.

[17] A. da Silva Soares and G. Latouche. Matrix-analytic methods for fluid queues with finite buffers. *Performance Evaluation*, 63(4-5):295 – 314, 2006.

[18] A. I. Elwalid and D. Mitra. Analysis and design of rate-based congestion control of high speed networks, i: stochastic fluid models, access regulation. *Queueing systems*, 9:29–63, 1991.

[19] M. Gribaudo and M. Telek. Fluid models in performance analysis. In M. Bernardo and J. Hillston, editors, *Formal methods for Performance Evaluation*, LNCS 4486, pages 271–317. Springer, 2007.

[20] J. Heinanen and R. Guerin. Rfc2698: A two rate three color marker, 1999.

[21] I. Horváth, G. Horváth, S. A.-D. Almousa, and M. Telek. Numerical inverse Laplace transformation using concentrated matrix exponential distributions. *Performance Evaluation*, 2019.

[22] D. P. Kroese and W. R. Scheinhardt. Joint distributions for interacting fluid queues. *Queueing systems*, 37:99–139, 2001.

[23] V. G. Kulkarni. Fluid models for single buffer systems. In J. H. Dshalalow, editor, *Models and Applications in Science and Engineering*, Frontiers in Queueing, pages 321–338. CRC Press, 1997.

[24] G. Latouche and P. G. Taylor. A stochastic fluid model for an ad hoc mobile network. *Queueing systems*, 63:109–129, 2009.

[25] M. Neuts. *Matrix Geometric Solutions in Stochastic Models*. Johns Hopkins University Press, Baltimore, 1981.

[26] M. M. O'Reilly and W. Scheinhardt. Analysis of tandem fluid queues. In *Proceedings of the Ninth International Conference on Matrix-Analytic Methods in Stochastic Models*, pages 85–92, 2016.

[27] V. Ramaswami. Matrix analytic methods for stochastic fluid flows. In *International Teletraffic Congress*, pages 1019–1030, Edinburg, 1999.